Spectrochimica Acta Part A: Molecular and Biomolecular Spectroscopy 97 (2012) 606–615

Contents lists available at SciVerse ScienceDirect

Spectrochimica Acta Part A: Molecular and Biomolecular Spectroscopy

journal homepage: www.elsevier.com/locate/saa

6-Phenyl-3-(4-pyridyl)-1,2,4-triazolo-[3,4-b][1,3,4]thiadiazole: Synthesis, experimental, theoretical characterization and biological activities

Ahmet Cansız [a], Ahmet Cetin [b,*], Cahit Orek [a], Mustafa Karatepe [a], Kamiran Sarac [c], Alper Kus [a], Pelin Koparir [d]

[a] Firat University, Faculty of Science, Department of Chemistry, 23119 Elazığ, Turkey
[b] Bingöl University, Faculty of Science, Department of Chemistry, 12100 Bingöl, Turkey
[c] Inönü University, Faculty of Science, Department of Chemistry, 44100 Malatya, Turkey
[d] Department of Chemistry, Forensic Medicine Institute, TR-44000 Malatya, Turkey

HIGHLIGHTS

- 6-Phenyl-3-(4-pyridyl)-1,2,4-triazolo-[3,4-b][1,3,4]thiadiazole was prepared.
- Synthesis compound was confirmed by IR, NMR and X-ray single-crystal diffraction.
- Comparison between HF and B3LYP levels of theory with 6-31G(d) basis set reported.
- Experimental parameters of title compound were compared with calculated parameters.
- The title compound has been tested in vitro for biological effects.

GRAPHICAL ABSTRACT

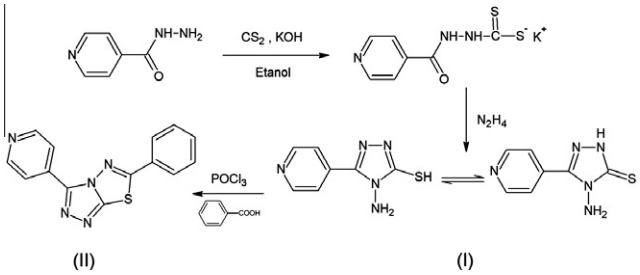

ARTICLE INFO

Article history:
Received 2 May 2012
Received in revised form 6 June 2012
Accepted 5 July 2012
Available online 16 July 2012

Keywords:
6-Phenyl-3-(4-pyridyl)-1,2,4-triazolo-[3,4-b][1,3,4]thiadiazole
DFT
HF
NMR
IR spectra
Biological effects

ABSTRACT

The molecular geometry, vibrational frequencies, and gauge including atomic orbital (GIAO) ^{1}H and ^{13}C NMR chemical shift values of the title compound in the ground state have been calculated using the Hartree–Fock (HF) and density functional theory (DFT) methods with 6-31G(d) basis sets, and compared with the experimental data. The calculated results show that the optimized geometries can well reproduce the crystal structural parameters and the theoretical vibrational frequencies, and ^{1}H and ^{13}C NMR chemical shift values show good agreement with experimental data. To determine conformational flexibility, molecular energy profile of the title compound was obtained by HF/6-31G(d) and (DFT/B3LYP) calculations with respect to selected degree of torsional freedom, which was varied from −180° to +180° in steps of 10°. The energetic behavior of the title compound in solvent media was examined using the B3LYP method with the 6-31G(d) basis set by applying the Onsager and the polarizable continuum model (PCM). The results obtained with these methods reveal that the PCM method provided more stable structure than Onsager's method. The title compound has been tested in vitro for biological effects.

Introduction

It is well known that the thiadiazole nucleus possesses interesting biological properties such as antimicrobial [1–3], antiinflammatory [4–6], antituberculosis [7], antihypertensive [8,9], and anticancer [10] activities. Furthermore, the triazole nucleus [11–13] and the pyridine [14] unit have attracted special attention from chemists due to their attractive biological activities. Incorporating a pyridine ring into active compounds sometimes improves their biological or physiological activities [15]. Several heterocycles containing a thiadiazole or triazole moiety have been reported [1–20]; however, the synthesis of heterocyclic

* Corresponding author. Tel.: +90 426 237 00 00; fax: +90 426 237 00 10.
E-mail address: acetin74@yahoo.com.tr (A. Cetin).

1386-1425/$ - see front matter © 2012 Elsevier B.V. All rights reserved.
http://dx.doi.org/10.1016/j.saa.2012.07.016

systems containing a thiadiazole nucleus fused to a pyridine-substituted triazole ring has rarely been reported [21–23]. A combination of these three rings may have a variety of structural and biological activities.

4,5-Substituted products containing 1,2,4-triazole in their molecules seem to be suitable candidates for further chemical modifications and might be of interest as pharmacologically active compounds and ligands useful in coordination chemistry [24]. Derivatives of 4-amino-5-substituted 1,2,4-triazole were synthesized by intramolecular cyclization of 1,4-disubstituted thiosemicarbazides [25]. In addition there are some studies on electronic structures and thiol-thione tautomeric equilibrium of heterocyclic thione derivatives [26–30].

The aim of the present work was to describe and characterize the molecular structure, vibrational properties and chemical shifts on 6-phenyl-3-(4-pyridyl)-1,2,4-triazolo-[3,4-b][1,3,4]thiadiazole crystalline-structure. A number of papers have recently appeared in the literature concerning the calculation of NMR chemical shift (c.s.) by quantum-chemistry methods [31–36]. These papers indicate that geometry optimization is a crucial factor in an accurate determination of computed NMR chemical shifts. Moreover, it is known that the DFT (B3LYP) method adequately takes into account electron correlation contributions, which are especially important in systems containing extensive electron conjugation and/or electron lone pairs. However, considering that as molecular size increases, computing-time limitations are introduced for obtaining optimized geometries at the DFT level, it was proposed that the single-point calculation of magnetic shielding by DFT methods was combined with a fast and reliable geometry optimization procedure at the molecular mechanics level [36]. The gauge-including atomic orbital (GIAO) [37,38] method is one of the most common approaches for calculating nuclear magnetic shielding tensors. It has been shown to provide results that are often more accurate than those calculated with other approaches, at the same basis set size [39]. In most cases, in order to take into account correlation effects, post-Hartree–Fock calculations of organic molecules have been performed using (i) Moller–Plesset perturbation methods, which are very time consuming and hence applicable only to small molecular systems, and (ii) density functional theory (DFT) methods, which usually provide significant results at a relatively low computational cost [40]. In this regard, DFT methods have been preferred in the study of large organic molecules [41], metal complexes [42] and organometallic compounds [43] and for GIAO ^{13}C c.s. calculations [39] in all those cases in which the electron correlation contributions were not negligible.

In this study, the title compound is a novel compound synthesized firstly in our laboratories by us. We have calculated geometrical parameters, fundamental frequencies and GIAO ^{1}H and ^{13}C NMR c.s. values of the title compound in the ground state to distinguish the fundamental from the experimental ^{1}H c.s. values, vibrational frequencies and geometric parameters, by using the HF and DFT (B3LYP) methods with 6-31G(d) basis set. Besides the characterization of the title compound, the biological activities of the 6-phenyl-3-(4-pyridyl)-1,2,4-triazolo-[3,4-b][1,3,4]thiadiazole, such as antioxidant and antimicrobial activities, were investigated.

A comparison of the experimental and theoretical spectra can be very useful in making correct assignments and understanding the basic c.s.-molecular structure relationship. And so, these calculations are valuable for providing insight into molecular analysis. The properties of the structural geometry, electronic charge distribution, molecular electrostatic potential (MEP) and the thermodynamic properties for the title compound at the HF and DFT methods with 6-31G(d) basis set were studied. We also make comparisons between experiments and calculations.

Experimental

Synthesis and physical properties

Melting points were determined on a Thomas Hoover melting point apparatus and uncorrected, but checked by differential scanning calorimeter (DSC). The I.R. spectra were measured with Perkin–Emler Spectrum one FT–IR spectrophotometer. Electronic spectral studies were conducted on a Shimadzu model UV-1700 spectrophotometer in the wavelength 1100–200 nm. The ^{1}H and ^{13}C spectra were taken on Bruker AC-300 and Bruker AC-400 NMR spectrometer operating at 400 MHz for ^{1}H, 100 MHz for ^{13}C NMR. Compounds were dissolved in $CDCl_3$, DMSO and chemical shifts were referenced to TMS (^{1}H and ^{13}C NMR). Starting chemicals were obtained from Merck or Aldrich. The reactions for the synthesis of (I–II) are shown in Fig. 1.

Synthesis of 6-phenyl-3-(4-pyridyl)-1,2,4-triazolo-[3,4-b][1,3,4]thiadiazole (II)

To a mixture of 4-amino-5-(4-pyridyl)-4H-1,2,4-triazole-3-thiol, (**I**) (5 mmol, 0.965 g.) and benzoic acid (1 mmol, 0.61 g.) phosphorous oxychloride (27 mmol, 2.5 ml) was added and the resulting mixture heated under reflux for 8 h in a water bath. The excess phosphorous oxychloride was then distilled of and the residue was poured onto crushed ice while stirring. The resulting solid was washed with dilute sodium bicarbonate solution and then recrystallized from dimethylformamide. Yield 70%; m.p. 222–224 °C; IR ν (cm^{-1}): 3102–3011 (Ar—CH), 1601–1592 (C=C, C=N), 665 (C—S—C). ^{1}H NMR(400 MHz, DMSO-d_6, ppm): δ 8.07 (d, J = 7.03, 2H, *o*-Ar—CH), 7.62–7.69 (m, 3H, *m, p*-Ar—CH), 8.24 (dd, 2H, J = 6.23, 1.47, pyridine C—CH), 8.82 (d, J = 5.87, 2H, pyridine N—CH). ^{13}C NMR (100 MHz, DMSO-d_6, ppm): 168.36, 151.46, 144.39, 133.69, 133.07, 130.43, 130.20, 129.50, 128.08, 120.16.

In vitro antimicrobial activity

Isolated bacteria used in this study were obtained from the forensic medicine institute in Malatya. The clinical isolates (*Shigella dysenteriae, Escherichia coli, Proteus vulgaris, Serratia* spp., *Klebsiella*, *Pseudomonas aeruginosa, Staphylococcus aureus*) were grown in Mueller–Hinton Broth media for 24 h at 37 °C. Antimicrobial activities of the title compound was estimated by a Minimum Inhibitory Concentration (MIC, μg/mL) using a micro-broth dilution method and essentially following the guidelines of Hannan [44]. A stock solution of each antimicrobial in DMSO was prepared according to NCCLS guidelines [45]. The MIC was carried out in standard sterile 96 well flat bottom microtitre plates and the layout was designed so that each row covered the final antimicrobial dilution of 500–0.5 μg/mL with one control well. Using sterilized micropipette, a 40 μL of the selected antimicrobial with the correct concentration was added to each well and another well was loaded with the same volume of control (DMSO solvent). Then a 150 μL of Mueller Hinton media was added to all wells, followed by a 10 μL (10^8 cfu/mL) of the bacterial culture giving a final concentration of 5×10^7 cfu/mL of bacteria in the well. The plates were sealed and incubated at 37 °C under atmospheric conditions. After 24 h incubation the microtitre plates were read using the ELISA reader. The minimal concentration that has optical density less than that of the control was defined as the MIC.

DPPH free radical scavenging activity

Free radical scavenging activity of the title compound was determined by measuring the change in the absorbance of DPPH**.** (1,1-diphenyl-2-picrylhydrazylradical) at 517 nm spectrophotometrically.

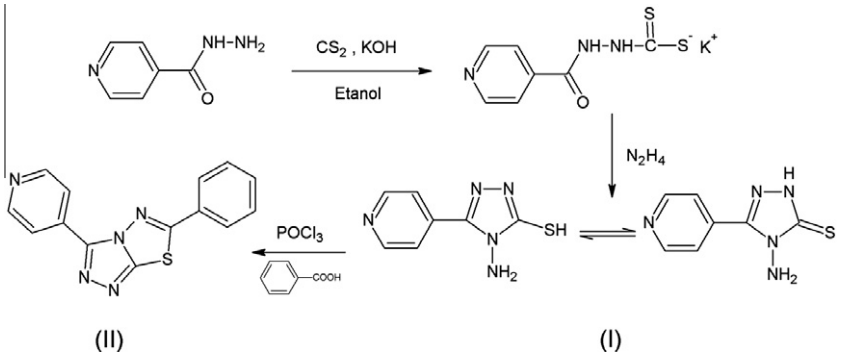

Fig. 1. Chemical structure for the title compound.

Stock solutions of 500 μM of tested sample and DPPH**.** were prepared in DMSO. Four-hundred microliters of DPPH**.** solution was added to sample solution at different concentrations (500, 1000, 1500, 2000 and 2500 μL) and appropriately diluted with DMSO to total volume of 4.0 mL. A 400 μL from DPPH**.** stock solution was also diluted to 4.0 mL using DMSO solvent to make the control. The reaction mixtures were thoroughly mixed by shaking the test tubes vigorously and incubated at 25 °C for 60 min in a water bath in the dark. Absorbance at 517 nm was measured and the solvent was corrected throughout. The scavenging effect was calculated using the following equation [46]:

$$\text{Scavenging activity } (\%) = \frac{A_0 - A_s}{A_0} \times 100$$

where A_s is the absorbance of the DPPH**.** in the presence of the tested compound and A_0 is the absorbance of the DPPH**.** in the absence of the tested compound (control). The data for antioxidation presented as means ± SD of three determinations.

Computational methods

Molecular geometry is restricted and all the calculations are performed without specifying any symmetry for the title molecule by using Gaussian 09W Program package [47] on a personal computer. The molecular structures of the title compound in the ground state (in vacuo) are optimized HF and B3LYP with 6-31G(d) basis set. Vibrational frequencies for optimized molecular structures have been calculated. Two sets of vibrational frequencies for these species are calculated with these methods and then scaled by 0.8929 and 0.9613, respectively [48]. The geometry of the title compounds, together with that of tetramethylsilane (TMS) is fully optimized. ^{1}H and ^{13}C NMR c.s. values are calculated within GIAO approach [37,38] applying B3LYP and HF method [49] with 6-31G(d) [50] basis set. The theoretical c.s. values of ^{1}H and ^{13}C were obtained by subtracting the GIAO isotropic magnetic shielding (IMS) values [51,52]. For instance, the average ^{13}C IMS of TMS are taken into account for the calculation of ^{13}C c.s. of any X carbon atom, and so c.s. can be calculated using the follow-

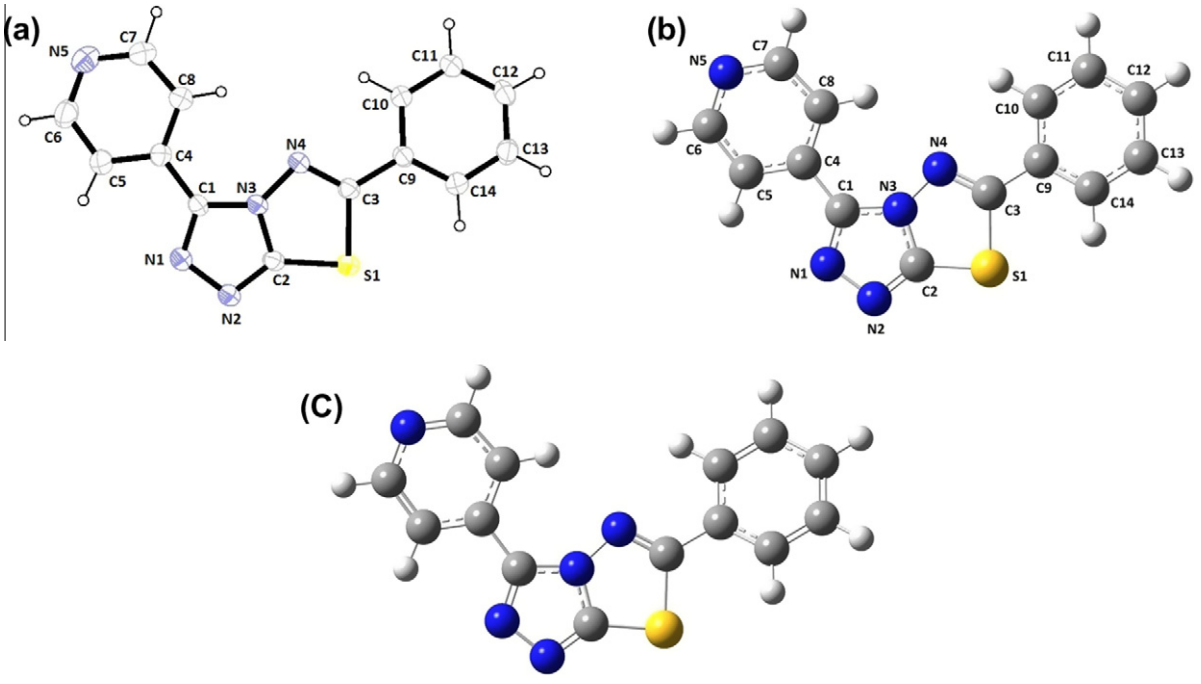

Fig. 2. (a) The experimental geometric structure of the title compound. (b) The theoretical geometric structure of the title compound (with B3LYP/6-31G(d) level). (c) The theoretical geometric structure of the title compound (with HF/6-31G(d) level).

Table 1
Crystallographic data for title compound [20].

Formula	$C_{14}H_9N_5S$
Formula weight	279.32
Temperature (K)	296
Crystal system	Monoclinic
Space group	$P2_{1/n}$
Unit cell	
a (Å)	11.3331(9)
b (Å)	5.4092(3)
c (Å)	20.3509(18)
β (°)	90.653(7)
V (Å^3)	1247.49(16)
z	4
D_{calc} (g/cm)	1.487
Crystal size	0.80 × 0.36 × 0.03 mm
Reflections observed [$I_o > 2D$ (I)]	1642
Data/parameters	2426/217
R [$F^2 > 2\sigma(F^2)$]	0.037
wR (F^2)	0.077
Goodness-of-fit on indicator	1.02
Structure determination	SHELX97
Refinement	Full matrix
(Ao) max, (Ao) min (e/A)	0.16, −0.21

ing equation $CS_x = IMS_{TMS} - IMS_x$. The effect of solvent on the theoretical NMR parameters was included using the default model Integral-Equation-Formalism Polarizable Continuum Model (IEF-PCM) [53] provided by Gaussian 09W. Dimethylsulfoxide (DMSO), with a dielectric constant (ε) of 46.7, was used as solvent.

A preliminary search of low-energy structures was carried out with the HF/6-31G(d) and (DFT/B3LYP) computations. Conformational energies were calculated as a one-dimensional scan by varying the φ_1(C8—C4—C1—N1) and φ_2(C10—C9—C3—S1) dihedral angles from −180° to +180° in steps of 10°, and the molecular energy profile was obtained. To investigate the total energy and dipole moment behavior of the title compound in solvent media, we also carried out optimization calculations in five solvents [$\varepsilon = 4.71$, chloroform ($CHCl_3$); $\varepsilon = 10.13$, dichloroethane (CH_2ClCH_2Cl); $\varepsilon = 24.85$, ethanol (C_2H_5OH); $\varepsilon = 46.83$, DMSO; $\varepsilon = 78.36$, water (H_2O)] at the B3LYP/6-31G(d) level using the Onsager [54] and polarizable continuum model (PCM) [55–58] methods. For the calculations of the MEP [59–62], using B3LYP/6-31G(d) level, was used. In addition, frontier molecular orbitals (FMO) and thermodynamic parameters for the title compound were performed with B3LYP/6-31G(d) the optimized structure.

Results and discussion

Crystal and molecular structure

The atomic numbering scheme for the title compound crystal [20] and the theoretical geometric structure of the title compound are shown in Fig. 2a–c. Fig. 2a is one ORTEP figure that shows the crystal structure of title compound. The B3LYP/6-31G(d) and HF/6-31G(d) optimized structure of title compound is illustrated in Fig. 2b and c. The crystal structure of the title compound is monoclinic and space group is $P2_{1/n}$, $M_w = 279.32$, $a = 11.3331$ (9) Å, $b = 5.4092$ (3) Å, $c = 20.3509$ (18) Å, $\beta = 90.653(7)$, and $V = 1247.49(16)$ Å^3, Dx = 1.487 g/cm^{-3}.

Additional information for the structure determinations are given in Table 1. The optimized parameters of the title compound (bond lengths and angles, and dihedral angles) by HF and B3LYP methods with 6-31G(d) as the basis set are listed in Table 2 and compared with the experimental crystal structure for the title compound. The four rings are almost coplanar. As expected, the 1,2,4-triazole and pyridine rings are planar, which can be attributed to a wide range of electron delocalization. The plane of the

Table 2
Selected optimized and experimental geometric parameters of 6-phenyl-3-(4-pyridyl)-1,2,4-triazolo-[3,4-b][1,3,4]thiadiazole ($C_{14}H_9N_5S$) in the ground state.

Parameters	Exp. [20]	Calculated	
		HF 6-31G(d)	B3LYP
Bond lengths (Å)			
C(1)–N(1)	1.318(2)	1.292	1.325
C(1)–N(3)	1.368(2)	1.365	1.382
C(2)–N(2)	1.312(2)	1.28	1.309
C(2)–N(3)	1.359(2)	1.347	1.374
C(2)–S(1)	1.724(2)	1.738	1.746
C(3)–N(4)	1.304(2)	1.27	1.302
N(1)–N(2)	1.395(2)	1.362	1.381
N(3)–N(4)	1.374(3)	1.358	1.364
C(6)–N(5)	1.327(2)	1.323	1.342
C(7)–N(5)	1.318(2)	1.318	1.338
C(9)–C(10)	1.390(2)	1.393	1.407
C(10)–C(11)	1.374(2)	1.381	1.391
C(11)–C(12)	1.379(4)	1.388	1.398
C(12)–C(13)	1.370(2)	1.384	1.396
RMSE[a]		0.016	0.012
Bond Angles (°)			
C(2)–N(2)–N(1)	105.47(2)	105.56	105.38
N(1)–C(1)–C(4)	125.56(2)	125.03	125.18
N(2)–C(2)–N(3)	111.14(2)	111.79	111.78
N(2)–C(2)–S(1)	139.24(2)	139.28	139.12
C(2)–S(1)–C(3)	87.59(9)	87.2	87.51
C(12)–C(13)–C(14)	120.71(2)	120.03	120.13
C(2)–N(3)–N(4)	118.42(1)	118.41	118.47
C(13)–C(14)–C(9)	120.07(2)	120.16	120.35
C(10)–C(11)–C(12)	120.40(2)	120.17	120.31
C(10)–C(9)–C(3)	119.54(2)	119.43	119.53
C(4)–C(5)–C(6)	118.99(2)	118.43	118.67
C(8)–C(4)–C(1)	123.05(1)	123.01	123.19
RMSE[a]		0.38	0.33
Dihedral angles (°)			
C(3)–S(1)–C(2)–N(2)	−179.5(2)	−179.93	−179.83
C(2)–S(1)–C(3)–N(4)	0.4(2)	−0.43	−0.3
N(2)–N(1)–C(1)–N(3)	−0.1(2)	0.1	0.08
C(2)–N(3)–C(1)–C(4)	179.3 (3)	179.92	179.91
C(8)–C(4)–C(5)–C(6)	−0.1(3)	0.05	0.04
N(1)–C(1)–C(4)–C(8)	−178.8(2)	174.71	179.04
S(1)–C(3)–C(9)–C(10)	171.9(1)	154.97	170.74

[a] Between the bond lengths and the bond angles computed by the theoretical method and those obtained from X-ray diffraction.

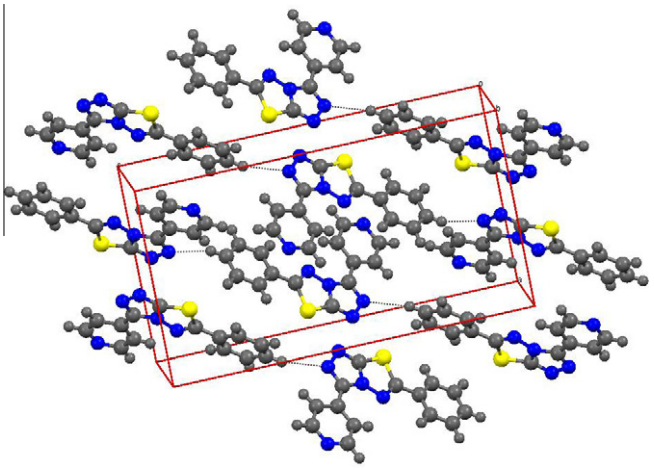

Fig. 3. Part of the crystal structure of the title compound, showing the intermolecular interactions (dashed lines). For the sake of clarity, H atoms not involved in the motifs shown have been omitted.

triazolo–thiadiazole system forms dihedral angles of 1.53 (13)° and 7.55 (12)° with the planes of the pyridine and phenyl rings,

Table 3
Hydrogen bonding geometry (Å,°) for the title compound.

D–H···A	D–H	H···A	D···A	D–H···A
C8–H8···N4	0.95 (2)	2.44 (2)	3.112(3)	128(2)
C14–H14···S1	0.97(2)	2.73 (2)	3.140(2)	106 (2)
C12–H12···N1[1]	0.94(2)	2.56(2)	3.452(3)	160 (2)

Symmetry code: (i) x−1/2, −y + ½, z + ½.

respectively. These dihedral angles have been found to be −5.34, −23.81° HF/6-31G(d) level and −0.96, −8.62° for B3LYP/6-31G(d) level. These experimental and theoretical results have shown coplanar of the title compound.

The crystal structure contain intermolecular C—H···N interactions. In the title compound, atom C12 in the molecule at (x, y, z) acts as hydrogen-bond donor, via atoms H12 to atoms N1 at $(x - 1/2, -y + 1/2, z + 1/2)$ (Fig. 3). The experimental C–H···N intermolecular contact distance value is 3.45 Å and bond angle value is 160°. The full geometry of intermolecular interactions is given in Table 3.

In order to compare the theoretical results with the experimental values, root mean square error (RMSE) is used. Calculated RMSE for bond lengths and bond angles are 0.016 Å and 0.38° for HF/6-31G(d) method and 0.012 Å and 0.33° for B3LYP/6-31G(d), respectively.

A logical method for globally comparing the structures obtained with the theoretical calculations is by superimposing the molecular skeleton with that obtained from X-ray diffraction, giving a RMSE of 0.170 Å for HF and 0.062 Å for B3LYP (Fig. S1). According to these results, it may be concluded that the DFT calculation well reproduce the geometry of the title compound.

The N1═C1 and N2═C2 bond distances (average = 1.315 (2) Å) are in good agreement with those found for structures containing the 1,2,4-triazole ring [63]. These distances have been calculated at 1.292, 1.280 Å for HF/6-31G(d) method and 1.325, 1.309 Å using B3LYP/6-31G(d) method, respectively. In (II), the presence of the pyridine ring in the 3-position of the triazole ring leads to an elongation of the N1-N2 bond length to 1.395 (2) Å. This bond is 1.371 (2) Å in 5-amino-3-trifluoromethyl-1H-1,2,4-triazole [64], in which an electron-withdrawing group is bound to the 3-position of the triazole ring. In present paper, we have calculated at 1.362 Å using HF/6-31G(d) method and 1.381 Å using B3LYP/6-31G(d) method and the data are shown in Table 2 for the optimized geometric parameters. The thiadiazole moiety displays differences in the pairs of bonds S1—C2/S1—C3 and C2—N3/C3—N4, due to the fused 1,2,4-triazole ring and the two different groups attached to either side of the triazolo–thiadiazole system. The difference between the S1—C2 [1.724 (2) Å] and S1—C3 [1.7651 (17) Å] bond distances indicates that the resonance effect caused by the triazole ring is stronger than that caused by the thiadiazole ring. The bond distances and angles of the pyridine ring are comparable with those in the literature [65]. In present work, according HF methods, the B3LYP method for optimized geometric parameters (bond lengths, bond and dihedral angles) is much closer to experimental data.

The molecular 1-D energy profiles with respect to rotations about the selected torsion angles are presented in Fig. 4. According to the results, the low-energy domains for φ_1(C8–C4–C1–N1) are located at −178.95°, −4.72° and 179.63° HF/6-31G(d) level and −178.95°, −1.31° and 176.63° for B3LYP/6-31G(d), having energy of −1205.093 and −1210.804 a.u., respectively, while they are located at −159.68°, −20.49°, 20.49° and 159.63° HF/6-31G(d) level and −179.63°, −9.98°, 9.20° and 178.95° for B3LYP/6-31G(d), having energy of −1205.093 and −1210.804 a.u., respectively for φ_2(C10–C9–C3–S1). Energy difference between the most favorable and unfavorable conformers, which arises from rotational potential barrier calculated with respect to the selected torsion angle, was

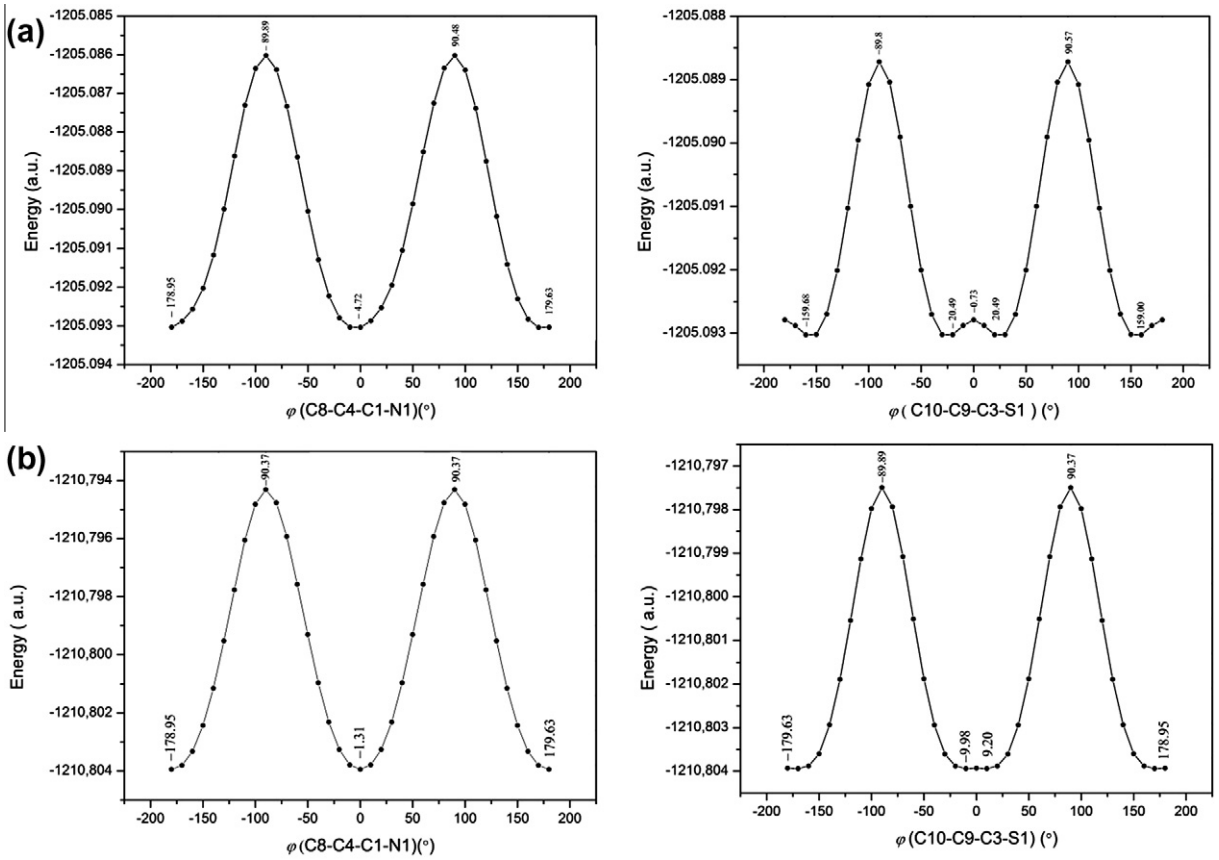

Fig. 4. Molecular energy profile against the selected torsional degree of freedom at (a) HF/6-31G(d) and (b) B3LYP/6-31G(d) level.

Table 4
Comparison of the observed and calculated vibrational spectra of 6-phenyl-3-(4-pyridyl)-1,2,4-triazolo-[3,4-b][1,3,4]thiadiazole ($C_{14}H_9N_5S$).

Assignments	FT-IR (cm^{-1}) with KBr	Scaled frequencies (6-31G(d)) (cm^{-1}) and relative intensity (I_{IR}, km/mol)) and relative intensity (I, km/mol)			
		B3LYP	I_{IR}	HF	I_{IR}
ν Pyridine C—H as.	3102	3112	0.01	3062	0.01
ν Pyridine C—H s.	3094	3111	0.01	3056	0.01
ν Benzene C—H s.	–	3107	0.02	3044	0.02
ν Benzene C—H s.	3086	3093	0.09	3033	0.07
ν Benzene C—H as.	3078	3083	0.07	3023	0.07
ν Benzene C—H as.	3070	3073	0.01	3014	0.11
ν Benzene C—H as.	–	3066	0.03	3013	0.02
ν Pyridine C—H s.	3054	3057	0.16	3008	0.12
ν Pyridine C—H as.	3011	3050	0.14	3006	0.00
α Benzene C=C	1601	1596	0.22	1627	0.34
α Pyridine C=C	1593	1592	0.42	1622	0.01
γ Benzene C=C	–	1576	0.00	1612	0.02
ν Pyridine N—C + γ C—H	–	1550	0.03	1587	0.01
ν N=C	1592	1518	0.10	1586	0.02
γ C—H + ν C—C	1510	1506	0.07	1551	0.42
ν N—C + γ C—H	1487	1481	0.02	1512	1.00
ν N=C + γ C—H	1463	1459	0.61	1492	0.10
ν N—C + γ C—H	1436	1430	1.00	1440	0.06
ν N—C + α C—C	1414	1405	0.05	1416	0.35
γ C—H	–	1321	0.02	1347	0.08
ν N—C	1274	1273	0.12	1268	0.07
ν N—C + ν C—C + γ C—H	1240	1258	0.08	1229	0.14
ν N—N + ν C—C + γ C—H	1217	1213	0.13	1198	0.01
α Pyridine C—H	–	1208	0.01	1168	0.02
α Benzene C—H	–	1173	0.04	1128	0.07
ν N—N + ν C—C	1099	1097	0.04	1093	0.04
α Benzene C—H	–	1077	0.4	1062	0.01
ν N—N + γ C—H	–	1029	0.08	1049	0.05
ν N—C—S	939	922	0.17	947	0.05
ω Pyridine C—H	821	818	0.10	845	0.10
ω Benzene C—H	756	750	0.14	768	0.13
ν Hetero-ring N—C—S	690	693	0.09	700	0.12
ω Benzene C—H	672	673	0.15	698	0.06
ν C—S—C	665	665	0.20	682	0.05
ν C—S—C	590	580	0.04	586	0.05
ω Pyridine C—H	518	516	0.03	526	0.03

ν, stretching; α, scissoring; γ, rocking; ω, wagging; s, symmetric; as, asymmetric.

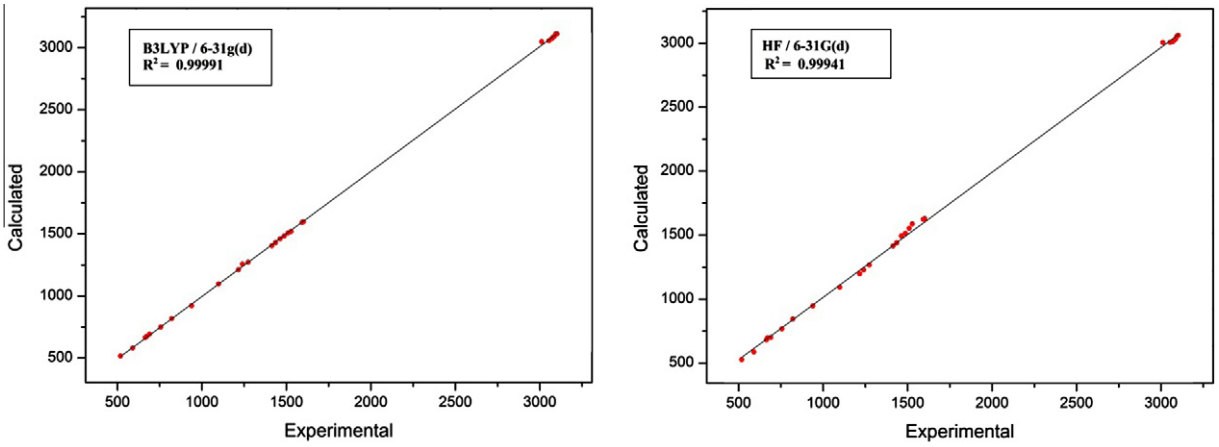

Fig. 5. Correlation graphics of calculated and experimental frequencies of the title compound.

calculated as 0.007 a.u. (for HF/6-31G(d)) and 0.006 a.u.(for B3LYP/6-31G(d)).

Assignments of the vibration modes

Harmonic vibrational frequencies of the title compound were calculated by using both HF and DFT (B3LYP) method with 6-31G(d) basis set. Two sets of vibrational frequencies for these species are calculated with these methods and then scaled by 0.8929 and 0.9613, respectively, by using Gauss-View [66] molecular visualization program; the vibrational bands assignments have been made. To facilitate assignment of the observed peaks, we have analyzed vibrational frequencies and compared our calculation of the title compound with their experimental results and shown in Table 4. The agreement between the experimental and calculated frequencies is quite good in general.

Table 5
Theoretical and experimental ^{13}C and ^{1}H isotropic chemical shifts (with respect to TMS, all values in ppm) 6-phenyl-3-(4-pyridyl)-1,2,4-triazolo-[3,4-b][1,3,4]thiadiazole ($C_{14}H_9N_5S$).

Atom	Experimental (ppm) (DMSO-d_6)	Calculated chemical Schift (ppm)	
		HF	B3LYP
C1	133.87	144.38	140.38
C2	151.48	154.71	154.4
C3	168.36	170.4	160
C4	133.07	136.42	127.83
C5	120.6	118.05	114.57
C6	144.39	149.42	144.27
C7	144.39	150.05	144.86
C8	120.6	118.08	114.3
C9	129.5	126.02	123.48
C10	128.09	128.22	121.15
C11	130.49	127.26	123.48
C12	133.07	134.22	128.11
C13	130.49	127.14	123.79
C14	128.09	129.29	123.2
2H (*o*-Ar—CH)	8.07	8.18 and 8.79	7.68 and 8.37
3H (m,p-Ar—CH)	7.62–7.69	8.01, 8.04 and 8.21	7.59, 7.62 and 7.66
2H (pyridine C—CH)	8.24	8.66 and 8.73	8.24 and 8.32
2H (pyridine N—CH)	8.82	9.21 and 9.25	8.76 and 8.80

Table 6
Minimum inhibitory concentration (MIC, μg/mL) data of the title compound against a number of bacteria.

Tested compound (MIC, μg/mL)	Gram (−) bacteria						Gram (+) bacteria
	Sd	*Ps*	*Pv*	*E. coli*	*Serratia*	*Klebsiella*	*Sa*
Title compound	N	62.5	N	62.5	N	N	N
Cephalexin	7.8	125	125	15.6	125	7.8	7.8
Cephradine	15.6	125	125	15.6	125	15.6	7.8

Sa, Staphylococcus aureus; *Ps, Pseudomonas aeruginosa*, *E. coli, Escherichia coli*; *Sd*, *Shigella dysenteriae*; *Pv*, *Proteus vulgaris*.
Cephalexin and cephradine are standard antibiotics.
N, non detected.

Table 7
Antioxidant scavenging activity data of the title compound on DPPH• free radical at different concentrations.

Tested compound	DPPH scavenging activity (%)	
	62.5 μM	125 μM
Title compound	40.7 ± 0.4	42.2 ± 0.1

Table 8
Total energies and dipole moments of the title compound in different solvent.

Method	ε	Energy (a.u.)	ΔE (kcal mol^{-1})	μ (D)
B3LYP	1	−1210.803942		7.1985
Onsager	4.71	−1210.807531	−2.2524	9.1967
	10.13	−1210.808534	−2.8815	9.7596
	24.85	−1210.80915	−3.2682	10.107
	46.83	−1210.809366	−3.4039	10.2293
	78.36	−1210.809468	−3.4677	10.2867
PCM	4.71	−1210.81349	−5.9917	8.7196
	10.13	−1210.81567	−7.3598	9.0482
	24.85	−1210.816932	−8.1517	9.2354
	46.83	−1210.817362	−8.4217	9.2987
	78.36	−1210.817562	−8.5471	9.328

$\Delta E = E_{solvation} - E_{gas}$, ε = dielectric constant.

The bands calculated in the measured region 4000–400 cm^{-1} arise from the vibrations of Ar—H, C=C, C=N, N—C—S stretching, the internal vibrations, etc., of the title compound. Most bands observed in infrared spectra of the title compound belong to aromatic groups modes, only some of them may be assigned to group ring C—H (symmetric/asymmetric) and C—C stretching bands were observed to be 3102–3011 and 1601–1510 as experimentally and compares well with the value reported previously [3111–3059, 1601–1494 cm^{-1}] [67].

These modes have been calculated at 3062–3006 and 1627–1551 cm^{-1} for HF/6-31G(d) level, 3112–3050 and 1596–1506 cm^{-1} for B3LYP/6-31G(d) level and compares well with the value reported previously [3021–2988 and 1624–1494 cm^{-1} for HF/6-31G(d) level, 3082–3050 and 1607–1487 cm^{-1} for B3LYP/6-31G(d) level] [68].

In the triazolo-thiadiazole system, the C=N and C—S—C stretching modes were observed to be 1592, 665–590 cm^{-1} as experimentally and compares well with the value reported previously [1625,687 cm^{-1}] [69]. These modes were calculated at 1586 and 682–586 cm^{-1} for HF/6-31G(d), 1518 and 682–586 cm^{-1} for B3LYP/6-31G(d) level and compares well with the value reported previously [1650 and 581 cm^{-1} for HF/6-31G(d) level, and 1590 and 587 cm^{-1} for B3LYP/6-31G(d) level] [67,70]. Also, the other levels of calculations can be seen in Table 4. These results indicated some band shifts with regard to the different substituent-triazolo, thiadiazole ring. Any discrepancy noted between the observed and the calculated frequencies may be due to the two facts: one is that the experimental results belong to solid phase and theoretical calculations belong to gaseous phase; the other is that the calculations have been actually done on a single molecule contrary to the experimental values recorded in the presence of intermolecular interactions.

Calculated infrared intensity (Rel. intensity) allows determination of the strength of the transition. Note that experimental IR

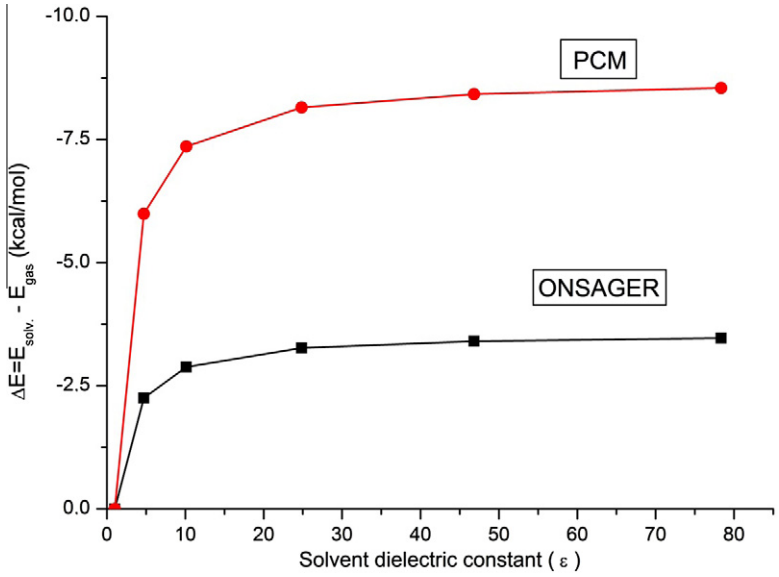

Fig. 6. Energy difference between the gas phase and solvent media by PCM and Onsager methods at B3LYP/6-31G(d) level of theory.

Table 9
Calculated energies (a.u.), zero-point vibrational energies (kcal mol^{-1}), rotational constants (GHz), entropies (cal mol^{-1} K^{-1}) and dipole moment (D) of the title compound.

Parameters	HF	B3LYP 6-31G(d)
Dipole moment (D)	7.3684	7.1985
Zero-point vibrational energy (kcal mol^{-1})	143.044	132.404
Total energy (a.u.)	−1205.0931	−1210.80394
Rotational constants	0.61352	0.60769
	0.18179	0.17944
	0.14139	0.13868
Entropy (cal mol^{-1} K^{-1})		
Rotational	34.277	34.318
Translational	42.777	42.777
Vibrational	46.293	50.605
Total	123.347	127.701

spectra are generally reported in either percent transmission or absorbance unit. Apparently, these mentioned can be seen in Fig. S2.

In Hartree–Fock, all the vibrational frequencies are overestimated and in agreement with the 10–20% error in the average of overall the frequencies [71,72]. To make comparison with experiment we present correlation graphic in Fig. 5 based on the calculations. As it can be seen from correlation graphic in Fig. 5, experimental fundamentals are in better agreement with the scaled fundamentals and are found to have better correlation for DFT than HF.

Assignments of the chemical shift values

DFT and HF methods differ in that no electron correlation effects are taken into account in HF. DFT methods treat the electronic energy as a function of the electron density of all electrons simultaneously and thus include electron correlation effect.

Explicitly, we have considered also of interest to investigate the influence of the level used for the geometry optimization on the final value of the title compound when GIAO ^{13}C and ^{1}H c.s. calculations have been performed. Thus, GIAO ^{13}C and ^{1}H c.s. calculations obtained at HF/6-31G(d) and B3LYP/6-31G(d) levels of theory for the three optimized geometries. The ^{13}C and ^{1}H c.s. values (with respect to TMS) have been calculated for the optimized structures of the title compound and generally compared to the experimental ^{1}H c.s. values.

These results are shown in Table 5. ^{13}C and ^{1}H c.s. values were experimentally observed, Therefore, ^{13}C and ^{1}H c.s values were only compared to theoretical results. We have calculated ^{1}H c.s. values (with respect to TMS) of 9.25–8.01 ppm with HF level and 8.80–7.59 ppm with B3LYP level., however, the experimental results were observed to be 8.82–7.62 ppm, these values are shown in Table 5, and so the accuracy ensures reliable interpretation of spectroscopic parameters.

As can be seen from Table 5, theoretical ^{1}H and ^{13}C c.s. results of the title compound are generally closer to the experimental c.s. data.

Biological study

Antimicrobial activity

The MIC of the title compound against different types of Gram-positive and Gram-negative bacteria were determined and tabulated in Table 6. The data indicate that the title compound showed moderate antimicrobial activity against *P. aereuginosa* and *E. coli* bacteria, and showed no activity towards *P. vulgaris*, *S. dysenteriae*, *S. aureus*, *Klebsiella* and *Serratia*.

Antioxidant activity

Since the antioxidants are gaining a lot of importance as panacea for a large number of life-style diseases like aging, cancer, diabetes, cardiovascular and other degenerative diseases, it is of immense significance to establish some new antioxidants by a convenient synthetic methodology.

Although a number of methods such as ORAC, ABTS, DMPD, FRAP, TRAP, TBA, superoxide radical scavenging, hydroxyl radical scavenging, nitric oxide radical scavenging, xanthine oxidase, cytochrome *C*, reducing power method, etc., available, the DPPH method is very common and proved as the best [73].

As shown in Table 7, the title compound has scavenging activity between 40.7% and 52.1% within the investigated concentration range. The antioxidant activity of the title compound is obvious that the scavenging activity increases with increasing sample concentration in the range tested.

Other molecular properties

Molecular electrostatic potential

Molecular electrostatic potential (MEP) is related to the electronic density and is a very useful descriptor in understanding sites for electrophilic attack and nucleophilic reactions as well as hydrogen bonding interactions [74–76]. The electrostatic potential $V(r)$ is also well suited for analyzing processes based on the "recognition" of one molecule by another, as in drug–receptor, and enzyme–substrate interactions, because it is through their potentials that the two species first "see" each other [77,78]. To predict reactive sites for electrophilic attack for the title compound, MEP was calculated at the B3LYP/6-31G(d) optimized geometry. The negative (red) regions of MEP were related to electrophilic reactivity and the positive (blue) ones to nucleophilic reactivity shown in Fig. S3. As easily can be seen in Fig. S3, this molecule has two possible sites for electrophilic attack. The negative regions are mainly over the N1, N2 and N5 atom. For the title compound, negative regions were calculated: the MEP value around N1 and N2 is more negative than that of N5 atom. Thus, the calculations suggested that the preferred site for electrophilic attack is the N1 and N2 atoms, followed from the N5 atom.

Total energies, dipole moments and frontier molecular orbitals

To evaluate the energetic behavior of the title compound in solvent media, we carried out calculations in five kinds of solvent ($\varepsilon = 78.39$, H_2O; $\varepsilon = 46.7$, DMSO; $\varepsilon = 24.55$, C_2H_5OH; $\varepsilon = 10.36$, CH_2ClCH_2C1; $\varepsilon = 4.9$, $CHC1_3$). Total energies and dipole moments were calculated in solvent media at B3LYP/6-31G(d) level using Onsager and PCM models and the results are presented in Table 8. According to Table 8, we can conclude that the total energies of the title compound obtained by Onsager and PCM methods decrease with the increasing polarity of the solvent, while the stability of the title compound increases in going from the gas phase to the solution phase. The energy difference between the gas phase and solvent media is given in Fig. 6 for both methods. As can be seen from Fig. 6, the PCM method provided a more stable structure than Onsager's method (4.6 kcal/mol on average).

The frontier molecular orbitals play an important role in the electric and optical properties, as well as in UV–Vis spectra and chemical reactions [79]. Fig. S4 shows the distributions and energy levels of the HOMO, HOMO−1, LUMO and LUMO+1 orbitals computed at the B3LYP/6-31G(d) level for the title compound.

The calculations indicate that the title compound has 72 occupied molecular orbitals. Both the highest occupied molecular orbitals (HOMOs) and the lowest-lying unoccupied molecular orbitals (LUMOs) are mainly localized on the rings indicating that the HOMO–LUMO are mostly the π-antibonding type orbitals. As seen from Fig. S4, in the HOMO−1 and HOMO, electrons are mainly delocalized on the pyridine and the triazole rings. However, when electron transitions take place, some electrons will enter into the LUMO and LUMO+1, then, in the LUMO and LUMO+1, the electrons will mainly be delocalized on thiadiazole and pyridine rings. Namely, electron transitions are corresponding to the $n \rightarrow \pi^*$ and $\pi \rightarrow \pi^*$ electron transitions. The value of the energy separation between the HOMO and LUMO is 4.2339 eV and this large energy gap indicates that the title structure is quite stable.

Thermodynamic parameters of the title compound

Several thermodynamic parameters were calculated using HF and B3LYP with 6-31G(d) basis set and calculated these parameters of the title compound are given in Table 9. Accurate prediction of zero-point vibrational energy (ZPVE) and the entropy ($S_{vib}(T)$) scaling the data [71]. The total energies and the change in the total entropy of the title compound at room temperature at different theoretical methods were also presented in Table 9 demonstrates several thermodynamic parameters of the title compound without of results of experimental.

Conclusions

In this study, 6-phenyl-3-(4-pyridyl)-1,2,4-triazolo-[3,4-b][1,3,4]thiadiazole was prepared following the reaction sequences depicted in Fig. 1. In the present study, the new compound 6-phenyl-3-(4-pyridyl)-1,2,4-triazolo[3,4-b][1,3,4]thiadiazole, (II), was synthesized in 70% yield by the reaction of 4-amino-5-(4-pyridyl)-4H-1,2,4-triazole-3-thiol, (I), benzoic acid and phosphorous oxychloride. The synthesis compound was confirmed by IR, NMR and X-ray single-crystal diffraction [20]. NMR spectrum of the title compound is shown in Fig. S5.

The comparisons between to test the different HF and B3LYP levels of theory with 6-31G(d) basis set reported, computed and experimental the geometric parameters, vibrational frequencies and chemical shifts of the title compound were compared. Thus, we scaled the data to fit the theoretical frequencies results with experimental ones for HF and B3LYP methods. Scaled results seemed to be in a good agreement with experimental ones. It is seen from the theoretical results, the results of DFT method showed a better fit to experimental ones than HF in evaluating geometrical parameters and vibrational frequencies, and chemical shifts. The antimicrobial activity results show that title compound possessed moderate antibacterial activity. The antioxidant activity of the title compound is obvious that the scavenging activity increases with increasing sample concentration in the range tested.

Appendix A. Supplementary data

Supplementary data associated with this article can be found, in the online version, at http://dx.doi.org/10.1016/j.saa.2012.07.016.

References

[1] K. Desai, A.J. Baxi, Indian J. Pharm. Sci. 54 (1992) 183–188.
[2] N.G. Gawande, M.S. Shingare, Indian J. Chem. 26B (1987) 387–389.
[3] M.G. Mamolo, L. Vio, E. Banfi, Farmaco 51 (1996) 71–74.
[4] M.D. Mullican, M.W. Wilson, D.T. Connor, C.R. Kostlan, D.J. Schrier, R.D. Dyer, J. Med. Chem. 36 (1993) 1090–1099.
[5] Y. Song, D.T. Connor, A.D. Sercel, R.J. Sorenson, R. Doubleday, P.C. Unangst, B.D. Roth, V.G. Beylin, R.B. Gilbertsen, K. Chan, D.J. Schrier, A. Guglietta, D.A. Bornemeier, R.D. Dyer, J. Med. Chem. 42 (1999) 1161–1169.
[6] L. Labanauskas, V. Kalcas, E. Udrenaite, P. Gaidelis, A. Brukstus, A. Dauksas, Pharmazie 56 (2001) 617–619.
[7] H.K. Shucla, N.C. Desai, R.R. Astik, K.A. Thaker, J. Indian Chem, Soc. 61 (1984) 168–171.
[8] S. Turner, M. Myers, B. Gadie, A.J. Nelson, R. Pape, J.F. Saville, J.C. Doxey, T.L. Berridge, J. Med. Chem. 31 (1988) 902–906.
[9] S. Turner, M. Myers, B. Gadie, S.A. Hale, A. Horsley, A.J. Nelson, R. Pape, J.F. Saville, J.C. Doxey, T.L. Berridge, J. Med. Chem. 31 (1988) 907–913.
[10] J.Y. Chou, S.Y. Lai, S.L. Pan, G.M. Jow, J.W. Chern, J.H. Guh, Biochem. Pharmacol. 66 (2003) 115–124.
[11] N.F. Eweiss, A.A. Bahajaj, E.A. Elsherbini, J. Heterocyclic Chem. 2 (1986) 1451–1458.
[12] M. Moreno-Mañas, Y. Arredondo, R. Pleixats, M. Teixidò, M.M. Haga, C. Palacin, J.M. Castellò, J.A. Ortiz, J. Heterocyclic Chem. 29 (1992) 1557–1560.
[13] J.B. Liu, W.F. Tao, H. Dai, Z. Jin, J.X. Fany, J. Heteroatom Chem. 19 (2007) 376–380.
[14] A. Mobinikhaledi, K.H. Zamani, R. Iqbal, T. Tofighi, J. Chem. Soc. Pakistan 24 (2002) 269–274.
[15] S. Mavel, J.L. Renou, C. Galtier, H. Allouchi, R. Snoeck, G. Andrei, E.D. Clercq, J. Gueifier, Bioorg. Med. Chem. Lett. 10 (2002) 941–946.
[16] M. Ahmedzade, A. Cukurovali, M. Koparir, J. Chem. Soc. Pakistan 25 (2003) 51–55.
[17] M. Koparir, A. Cansiz, M. Ahmedzade, A. Cetin, Heteroatom Chem. 15 (2004) 26–31.
[18] O.F. Ozturk, A. Cansiz, M. Koparir, Transit. Metal Chem. 32 (2007) 224–227.
[19] S. Ozturk, M. Akkurt, A. Cansiz, M. Koparir, M. Sekerci, F.W. Heinemann, Acta Cryst. E 60 (2004) o820–o821.

[20] M. Dincer, N. Ozdemir, A. Cetin, T. Keser, O. Buyukgungor, Acta Cryst. C 62 (2006) o639–o642.
[21] M. Koparir, P. Koparir, A. Cansiz, M.M. Temuz, Asian J. Chem. 22 (2010) 6059–6066.
[22] R.J. Singh, D.K. Singh, S. Afr, J. Chem. 62 (2009) 105–108.
[23] N. Foroughifar, A. Mobinikhaledi, S. Ebrahimi, M.A. Bodaghi Fard, H. Moghannian, J. Chin. Chem. Soc. 56 (2009) 1043–1047.
[24] O. Kahn, C. Martinez, J. Sci. 279 (1998) 44–48.
[25] M. Koparir, A. Cetin, A. Cansiz, Molecules 10 (2005) 475–480.
[26] S. Ozturk, M. Akkurt, A. Cansiz, M. Koparir, M. Sekerci, F.W. Heinemann, Acta Crystallogr. E 60 (2004) o425–o427.
[27] S. Ozturk, M. Akkurt, A. Cansiz, M. Koparir, M. Sekerci, F.W. Heinemann, Acta Crystallogr. E 60 (2004) o642–o644.
[28] A. Cansiz, A. Cetin, P. Kutulay, M. Koparir, Asian J. Chem. 21 (2009) 617–626.
[29] S.O. Yıldırım, M. Akkurt, A. Cetin, A. Cansiz, M. Sekerci, F.W. Heinemann, Anal. Sci. 21 (2005) x121–x122 (X-ray Structure Analysis Online).
[30] S.O. Yildirim, M. Akkurt, M. Koparir, A. Cansiz, M. Sekerci, F.W. Heinemann, Acta Crystallogr. E 60 (2004) o2368–o2370.
[31] J. Casanovas, A.M. Namba, S. Leon, G.L.B. Aquino, G.V.J. Da Silva, C. Aleman, J. Org. Chem. 66 (2001) 3775–3782.
[32] A.B. Sebag, D.A. Forsyth, M.A. Plante, J. Org. Chem. 66 (2001) 7967–7973.
[33] D.B. Chesnut, in: K.B. Lipkowitz, D.B. Boyd (Eds.), Reviews in Computational Chemistry, vol. 8, VCH, New York, 1996, p. 245.
[34] A.C. De dios, Prog. Nucleic Magn. Reson. Spectrosc. 29 (1996) 229–278.
[35] D.A. Forsyth, A.B. Sebag, J. Am. Chem. Soc. 119 (1997) 9483–9494.
[36] T. Helgaker, M. Jaszunski, K. Ruud, Chem. Rev. 99 (1999) 293–352.
[37] R. Ditchfleld, J. Chem. Phys. 56 (1972) 5688–5691.
[38] K. Wolinski, J.F. Hinton, P. Pulay, J. Am. Chem. Soc. 112 (1990) 8251–8260.
[39] J.R. Cheeseman, G.W. Trucks, T.A. Keith, M.J. Frisch, J. Chem. Phys. 104 (1996) 5497–5509.
[40] P. Cimino, L. Gomez-Paloma, D. Duca, R. Riccio, G. Bifulco, Magn. Reson. Chem. 4 (2004) 26–33.
[41] R.A. Friesner, R.B. Murphy, M.D. Beachy, M.N. Ringnalda, W.T. Pollard, B.D. Dunietz, Y. Cao, J. Phys. Chem. A 103 (1999) 1913–1928.
[42] L. Rufisek, Z. Havlas, In. J. Quantum Chem. 91 (2003) 504–510.
[43] T. Ziegler, Chem. Mater. Sci. (1997) 69.
[44] G.L. Woods, J.A. Washington, Antibacterial susceptibility tests: dilution and disk diffusion methods, in: P.R. Murray, E.J. Baron, M.A. Pfaller, F.C. Tenover, R.H. Yolken (Eds.), Manual of Clinical Microbiology, sixth ed., American Society for Microbiology, Washington, DC, 1995, pp. 1327–1341.
[45] J. Roberts, The Cephalosporins in Kirk-Othmer Encyclopedia of Chemical Technology, vol. 3, John Wiley & Sons Inc., 1992.
[46] M.M. Hossain, M.F. Aziz, R. Ahmed, M. Hossain, A. Mahmuda, T. Ahmed, M.H. Mazumder, Int. J. Pharm. Sci. 2 (2010) 60–63.
[47] M.J. Frisch, G.W. Trucks, H.B. Schlegel, G.E. Scuseria, M.A. Robb, J.R. Cheeseman, G. Scalmani, V. Barone, B. Mennucci, G.A. Petersson, H. Nakatsuji, M. Caricato, X. Li, H.P. Hratchian, A.F. Izmaylov, J. Bloino, G. Zheng, J.L. Sonnenberg, M. Hada, M. Ehara, K. Toyota, R. Fukuda, J. Hasegawa, M. Ishida, T. Nakajima, Y. Honda, O. Kitao, H. Nakai, T. Vreven, J. A. Montgomery Jr., J.E. Peralta, F. Ogliaro, M. Bearpark, J.J. Heyd, E. Brothers, K.N. Kudin, V.N. Staroverov, R. Kobayashi, J. Normand, K. Raghavachari, A. Rendell, J.C. Burant, S.S. Iyengar, J. Tomasi, M. Cossi, N. Rega, J.M. Millam, M. Klene, J.E. Knox, J.B. Cross, V. Bakken, C. Adamo, J. Jaramillo, R. Gomperts, R.E. Stratmann, O. Yazyev, A.J. Austin, R. Cammi, C. Pomelli, J.W. Ochterski, R.L. Martin, K. Morokuma, V.G. Zakrzewski, G.A. Voth, P. Salvador, J.J. Dannenberg, S. Dapprich, A.D. Daniels, O. Farkas, J.B. Foresman, J.V. Ortiz, J. Cioslowski, D.J. Fox, Gaussian, Inc., Wallingford, CT, 2009.
[48] M.P. Andersson, P. Uvdal, J. Phys. Chem. A 109 (2005) 2937–2941.
[49] G. Rauhut, S. Puyear, K. Wolinski, P. Pulay, J. Phys. Chem. 100 (1996) 6310–6316.
[50] R. Ditchfield, W.J. Hehre, J.A. Pople, J. Chem. Phys. 54 (1971) 724–728.
[51] R. Ditchfleld, Mol. Phys. 27 (1974) 789–807.
[52] C.M. Rohlflng, L.C. Allen, R. Ditchfleld, Chem. Phys. 87 (1984) 9–15.
[53] E. Cances, B. Mennucci, J. Tomasi, J. Chem. Phys. 107 (1997) 3032–3041.
[54] L. Onsager, J. Am. Chem. Soc. 58 (1936) 1486–1493.
[55] S. Miertus, E. Scrocco, J. Tomasi, Chem. Phys. 55 (1981) 117–129.
[56] V. Barone, M. Cossi, J. Phys. Chem. A 102 (1998) 1995–2001.
[57] M. Cossi, N. Rega, G. Scalmani, V. Barone, J. Comput. Chem. 24 (2003) 669–681.
[58] J. Tomasi, B. Mennucci, R. Cammi, Chem. Rev. 105 (2005) 2999–3093.
[59] P. Politzer, S.J. Landry, T. Warnheim, Phys. Chem. 86 (1982) 4767, http://dx.doi.org/10.1021/j100221a024.
[60] P. Politzer, L. Abrahmsen, P. Sjoberg, J. Am. Chem. Soc 106 (1984) 855, http://dx.doi.org/10.1021/ja00316a005.
[61] P. Politzer, P.R. Laurence, L. Abrahmsen, B.A. Zilles, P. Sjoberg, Chem. Phys. Lett 111 (1984) 75, http://dx.doi.org/10.1016/0009-2614(84)8 0439-X.
[62] J.S. Murray, P. Lane, T. Brinck, P. Politzer, P. Sjoberg, J. Phys. Chem. 95 (1991) 14.
[63] S. Ozbey, N. Ulusoy, E. Kendi, Acta Crystallogr. C 56 (2000) o222–o224.
[64] O.Y. Borbulevych, O.V. Shishkin, S.M. Desenko, V.N. Chernenko, V.D. Orlov, Acta Crystallogr. C 54 (1998) 442–444.
[65] J. Ni, Y.Z. Li, W.B. Qi, Y.J. Liu, H.L. Chen, Z.L. Wang, Acta Crystallogr. C 59 (2003) o470–o472.
[66] A. Frisch, A.B. Nielsen, A.J. Holder, Gaussview User Manual, Gaussian Inc, Pittsburg, 2001.
[67] Y. Atalay, F. Yakuphanoglu, M. Sekerci, D. Avcı, A. Basoglu, Spectrochim. Acta A 64 (2006) 68–72.
[68] N. Ozdemir, M. Dincer, A. Cukurovalı, O. Buyukgungor, J. Mol. Model. 15 (2009) 1435–1445.
[69] S.N. Swamy, B.S. Basappa, P.B. Prabhuswamy, B.H. Doreswamy, J.S. Prasad, K.S. Rangappa, Eur. J. Med. Chem. 41 (4) (2006) 531–538.
[70] A. Cansiz, C. Orek, M. Koparir, P. Koparir, A. Cetin, Spectrochim. Acta A 91 (2012) 136–145.
[71] A.P. Scott, L. Radom, J. Phys. Chem. 100 (1996) 16502–16513.
[72] M.A. Palafox, M. Gill, N.J. Nunez, V.K. Rastogi, L. Mittal, R. Sharma, Int. J. Quant. Chem. 103 (2005) 394–421.
[73] V. Bondet, W. Brand-Williams, C. Berset, Lebensm. Wiss. Technol. 30 (1997) 609–615.
[74] E. Scrocco, J. Tomasi, Adv. Quantum Chem. 11 (1978) 115–193.
[75] F.J. Luque, J.M. Lopez, M. Orozco, Theor. Chem. Acc 103 (2000) 343–345.
[76] N. Okulik, A.H. Jubert, Internet Electron J. Mol. Des. 4 (2005) 17–30.
[77] P. Politzer, P.R. Laurence, K. Jayasuriya, J. McKinney, Environ. Health Perspect 61 (1985) 191–202.
[78] E. Scrocco, J. Tomasi, Topics in Current Chemistry, vol. 7, Springer, Berlin, 1973. p. 95.
[79] Fleming Frontier orbitals and organic chemical reactions. Wiley, London, 1976.